Electronic correlations in short-period $(CrAs)_n/(GaAs)_n$ ferromagnetic heterostructures

L. Chioncel,[1,2] I. Leonov,[3] H. Allmaier,[4] F. Beiuşeanu,[5] E. Arrigoni,[4] T. Jurcuţ,[5] and W. Pötz[6]

[1]*Augsburg Center for Innovative Technologies, D-86135 Augsburg, Germany*

[2]*Institute of Physics, University of Augsburg, D-86135 Augsburg, Germany*

[3]*Theoretical Physics III, Center for Electronic Correlations and Magnetism, Institute of Physics, University of Augsburg, D-86135 Augsburg, Germany*

[4]*Institute of Theoretical and Computational Physics, Graz University of Technology, A-8010 Graz, Austria*

[5]*Faculty of Science, University of Oradea, RO-47800 Oradea, Romania*

[6]*Institute of Theoretical Physics, Karl-Franzens University Graz, A-8010 Graz, Austria*

(Received 9 November 2010; published 13 January 2011)

We investigate half-metallicity in [001] stacked $(CrAs)_n/(GaAs)_n$ heterostructures with $n \leqslant 3$ by means of a combined many-body and electronic structure calculation. Interface states in the presence of strong electronic correlations are discussed for the case $n = 1$. For $n = 2,3$ our results indicate that the minority spin half-metallic gap is suppressed by local correlations at finite temperatures and continuously shrinks on increasing the heterostructure period. Although around room temperature the magnetization of the heterostructure deviates by only 2% from the ideal integer value, finite temperature polarization at E_F is reduced by at least 25%. Below the Fermi level the minority spin highest valence states are found to localize more on the GaAs layers while lowest conduction states have a many-body origin. Our results, therefore, suggest that in these heterostructures holes and electrons remain separated among different layers.

DOI: 10.1103/PhysRevB.83.035307 PACS number(s): 75.50.Cc, 71.10.Fd, 71.20.−b, 71.27.+a

I. INTRODUCTION

In recent years, the increasing ability to control the growth of semiconductor crystals has made possible the fabrication of high-quality artificial heterostructures of many different geometries and semiconductor classes. Heterostructures interfacing half-metals with semiconductors are technologically very attractive, since in principle they can be used to attain high polarization spin injection from a ferromagnetic electrode into the semiconductor. The high polarization results from the main property of half-metallic ferromagnets, namely the fact that they exhibit a metallic density of states for one spin channel and a gap at the Fermi level for the other.[1,2] The major players in the present semiconductor-based electronic technology are zinc-blende structures. For this reason, half-metals which can adapt to the structure and bonding of zinc-blende semiconductors are especially attractive as they are compatible with existing technology.

Recently, Zhao and Zunger[3] investigated the relative stability of NiAs and zinc-blende (ZB) structures under pseudomorphic epitaxial conditions. They found that under epitaxial growth condition, most of the Cr and Mn pnictides and chalcogenides cannot be stabilized below a lattice constant of 6.5 Å. However, these conclusions are valid for the growth of thick layers, whereas the growth of very thin films is dominated by the strain energy at the interface. This explains the experimental observation that CrAs can be grown in the zinc-blende structure for thicknesses up to a few monolayers.

The first experimental realization of such thin films was done by Akinaga *et al.*[4] In their work they have synthesized zinc-blende CrAs thin films of 3-nm thickness on GaAs substrates. They measured a magnetic moment of 3 μ_B, which is in agreement with theoretical prediction, and found an experimental Curie temperature above 400 K.[4] From the experimental point of view, such small thickness makes this material difficult to use in practical devices. Therefore, attention was directed toward CrAs/GaAs multilayers.[5] Previous *ab initio* calculations showed high spin polarization through the entire region of the multilayer in the case of two monolayer CrAs and two monolayer of GaAs stacked alternatively $(CrAs)_2/(GaAs)_2$.[6] Initially, the produced multilayers of zinc-blende CrAs/GaAs grown on GaAs substrates[5] indicated that the surface and interface of the multilayer were not completely flat. However, it was found that the multilayers grow much thicker than pure zinc-blende CrAs. Recently, by optimizing the growth temperature, the quality was improved significantly, and epitaxial growth of the zinc-blende multilayer with a flat surface and interface was achieved.[7] The magnetization measurements for a multilayer structure of $(CrAs)_2/(GaAs)_2$ repeated 100 times[7] showed a value of 2 μ_B per formula unit, lower than the theoretical prediction of 3 μ_B. In addition, the temperature dependence of magnetization indicated a ferromagnetic transition temperature of about 800 K. Moreover, it was confirmed by electronic structure calculations that the spin polarization is preserved throughout the multilayer and that it is insensitive to substitutional disorder between the Cr and Ga sites.[6]

It is the purpose of the present article to investigate effects caused by many-body correlations at finite temperatures in the short-period $(CrAs)_n/(GaAs)_n$ heterostructures. These *ab initio* calculations are performed within a combined density functional and many-body dynamical mean-field theory. Our results show that correlations do not affect much magnetization in these materials, while polarization is strongly suppressed. In particular, the minority spin gap contributes in confining the electrons and holes in the heterostructure, an effect similar to the one discussed for the $(GaAs)_n/(AlAs)_n$ superlattices where electrons and holes are spatially separated.[8]

The article is organized as follows: the microscopic description of electronic states around the half-metallic gap in bulk CrAs is briefly summarized in Sec. II. The geometry of

multilayers structures which results in lowering the symmetry are discussed in Sec. III. Results are presented in Sec. IV.

II. BAND-EDGE STATES IN HALF-METALLIC BULK CRAS

Before discussing the nature of the half-metallic gap in $(CrAs)_n/(GaAs)_n$ heterostructure with or without electron-electron interactions, let us briefly summarize the principal physical factors leading to gap formation in the zinc-blende bulk materials (Fig. 1).

Bulk properties of zinc-blende pnictides and chalcogenides were discussed in many articles.[9–12] In particular, first-principles calculations[4,13] predicted CrAs to be half metallic. In this structure every atom has a tetrahedral coordination with the first neighbors being of the other atomic species. d states split into the t_{2g} and e_g manifolds. While t_{2g} states hybridize with the p states of the neighboring atom, forming bonding and anti-bonding states, e_g orbitals are practically nonbonding and form narrow bands. The bonding-antibonding splitting is a characteristic of the tetrahedral coordination. The Fermi-level E_F is situated in the gap between the bonding bands and the narrow nonbonding e_g bands. In addition, the existence of the band gap is assisted by the exchange splitting which keeps minority e_g states higher in energy. A preliminary analysis of the electronic bands in the minority spin channel shows that the nature of the gap can change depending on the lattice parameter. For $a = 5.75$ Å, Fig. 2 shows a "direct gap" formed at the X point, while for $a = 6.06$Å the gap appears to have an "indirect" nature. In addition, we verified that states at the top of the valence band are p-d hybridized states, while states at the bottom of the conduction band (electrons) are predominantly Cr-d states. As one can see in Fig. 2 the entire manifold around

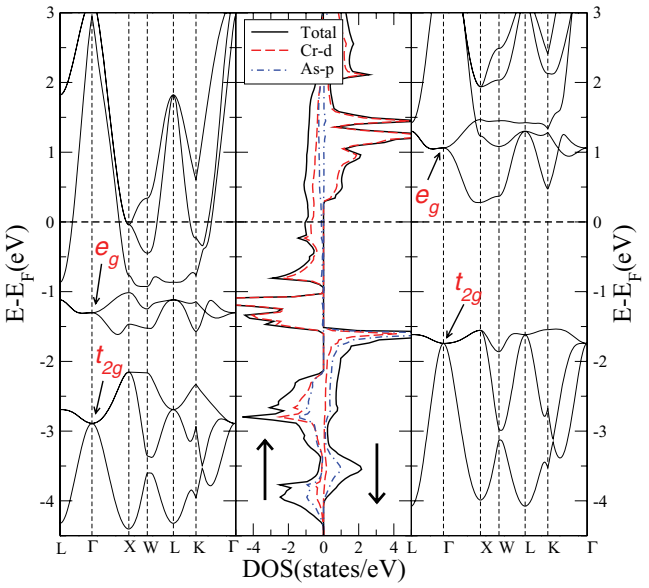

FIG. 1. (Color online) Local spin -density approximation (LSDA); total (black line) and atom resolved [Cr (red dashed line) As (blue dot-dashed line)] density of states for bulk CrAs with a lattice parameter $a = 5.75$ Å (central panel). Left and right panels display the majority and minority spin band structure, respectively. States with t_{2g} and e_g symmetry are indicated by an arrow at the Γ point.

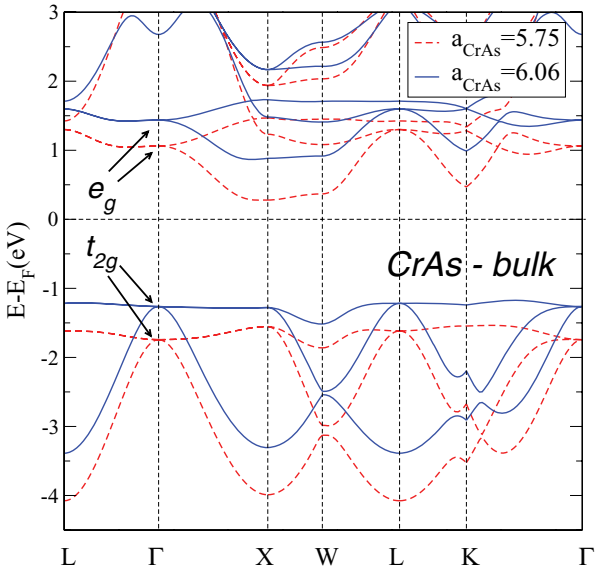

FIG. 2. (Color online) Minority spin bulk-CrAs band structure for the different lattice parameters: $a = 5.75$Aring; corresponding to an enlarged CrAs (red long dashed line), and $a = 6.06$ Å corresponding to the InAs lattice parameter (blue solid line). By increasing the lattice parameter the gap changes from a direct to an indirect one. Results obtained from an LSDA calculation.

the Fermi level is shifted to higher energies as the lattice parameter is increased. Such changes in the lattice parameter may occur when the half-metal is grown on a semiconductor substrate.

Electronic structure calculations for bulk CrAs for different lattice constants at finite temperatures and including correlation effects were performed recently by one of the authors.[14] It was shown that correlations induce spectral weight in the minority spin gap, while the material remains half-metallic. The spectral weight in the minority spin gap is known as so-called nonquasiparticle (NQP) states. The occurrence of these states is connected to "spin-polaron" processes: the spin-down low-energy electron excitations, which are forbidden for half-metallic ferromagnets in the one-particle picture, turn out to be possible as superpositions of spin-up electron excitations and virtual magnons.[15,16] It is important to mention that the only situation in which half-metallicity is preserved in the presence of finite temperature correlations is in CrAs and VAs, while in other (semi-)Heusler materials the additional spectral weight builds up at the Fermi energy, so that strong depolarization takes place.[17–19] Depolarization can originate from other effects, such as spin-orbit coupling, which causes a mixing of the two spin channels. However, in CrAs this effect was found to be less than 1%.[20] Consequently, this interaction is not taken into account for the present calculations.

There is an enormous amount of literature on GaAs band-structure calculations, all showing a direct gap at the Γ point in the band structure. The general discussion is focused on the difficulty of density-functional theory (DFT) mean-field type calculations based on the local-density approximation (LDA)/generalized-gradient approach (GGA) to reproduce the magnitude of the experimental gap which is around 1 eV. It has been assumed that the band gap problem does not occur in half-metals since their dielectric response is that of a metal.

This assumption was recently contradicted by a GW type of calculation for $La_{0.7}Sr_{0.3}MnO_3$, which predicts a half-metallic band gap that is 2 eV larger than the one obtained by DFT.[21] In particular, for the present case of semiconducting and half-metal heterostructures this might imply that the DFT gaps might underestimate the actual experimental values.

In the present work we investigate the nature of the minority spin states involved in the gap formation of $(CrAs)_n/(GaAs)_n$ heterostructures. In our analysis the CrAs bulk states situated at the X point play a crucial role because by Brillouin zone folding associated with symmetry lowering present in the $(CrAs)_n/(GaAs)_n$ heterostructure, the X point is folded into the Γ point, where the bottom of the conduction band in GaAs is expected to be present. Therefore, the relative position of the states in the X point with respect to the bottom of the GaAs conduction band would contribute to the band-edge states. This effect will be discussed in detail in the next sections. Moreover, we investigate up to what extent the electronic states forming the $(CrAs)_n/(GaAs)_n$ band structure are significantly changed by finite-temperature dynamic correlations.

III. MULTILAYERS GEOMETRY AND METHOD OF CALCULATION

The $(CrAs)_n/(GaAs)_n$ heterostructure, with $n \leqslant 3$, extends along the [001] direction of the of bulk zinc-blende material. The unit cells of the superlattice having the space group symmetry D^1_{2d} are simple tetragonal with $c/a_0 = 2n/\sqrt{2}$, where c is the unit-cell dimension along the stacking direction. The basis of the tetragonal cell have the constants $a = b = a_0/\sqrt{2}$, where a_0 represents the FCC lattice parameter. The positions of the atoms in the $(CrAs)_1/(GaAs)_1$ unit supercell are Cr:$a/2(0,0,0)$, As:$a/2(0,1,c/a)$, Ga:$a/2(1,1,c/a)$, and As:$a/2(1,0,3c/2a)$ (see Fig. 3). In the heterostructure calculations we included empty spheres with no net nuclear charge in the empty tetrahedral sites in order to obtain a close-packed structure, as it is generically done for zinc-blende semiconductors. For the $(CrAs)_1/(GaAs)_1$ case the empty spheres surrounding the cations and anions are located at $a/2(1,0,3c/2a)$, $a/2(0,1,c/2a)$, $a/2(0,0,c/a)$, $a/2(1,1,0)$. The positions of the atoms in larger unit cells for the other superlattices can be written by extrapolating the $(CrAs)_1/(GaAs)_1$ case.

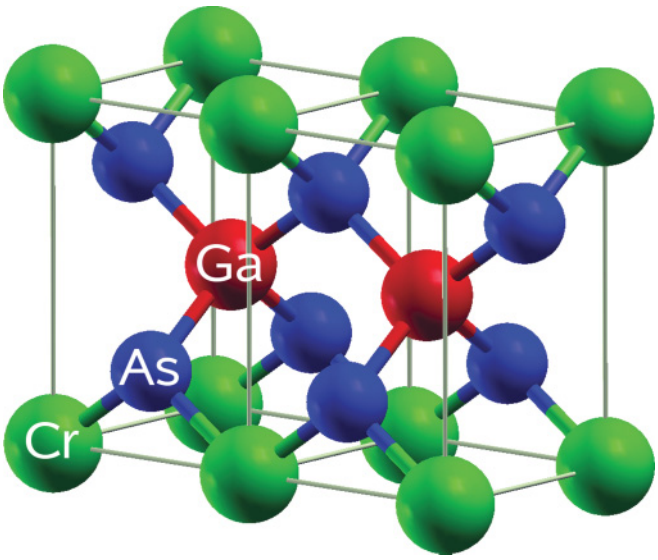

FIG. 3. (Color online) $(CrAs)_1/(GaAs)_1$ supercell, which is repeated twice along the x axis for illustrative purposes. Atoms situated in different symmetry positions are presented by colored spheres, Cr (green), lower and upper planes; As (blue), above and below the Cr layers, and Ga (red), center of the unit cell.

Similar supercells were considered previously in discussing the electronic structure of semiconducting $(GaAs)_m/(AlAs)_n$ superlattices.[8] For the particular case when $m = n$ it was demonstrated that within the tetragonal Brillouin zone the X point (along the $\mathbf{k}_z$ direction) of the FCC zone folds onto the Γ point. On increasing the number of layers in the superlattice, the Brillouin zone is compressed along $\mathbf{k}_z$ and the number of zone foldings increase. Contrary to the bulk semiconductors where the top of the valence band is mainly As-p like states, in the case of $(GaAs)_m/(AlAs)_n$ heterostructures As-p anionic bonds are shared between Ga and Al atoms, leading to confinement effects at the valence band maxima.

For the case of $(CrAs)_n/(GaAs)_n$ heterostructures the As-p states are shared by Ga and Cr atoms. In particular, due to hybridization the Cr-d states contribute significantly to the top of the minority spin valence band. Therefore, in addition to the confining effect determined by the dimensionality of the heterostructure, electronic correlation are expected to influence the minority spin band-edge states around the gap.

In our calculations we used the lattice parameter $a_0 = 5.75$ Å, which is the optimized GaAs lattice constant obtained from a spin-GGA calculation.[22] This value is slightly larger than the one found experimentally for GaAs ($a_0 = 5.65$ Å) and the one predicted for $(CrAs)_2/(GaAs)_2$ double monolayers ($a_0 = 5.69$ Å).[6] We checked that our results do not change when the atomic sphere radii are chosen to be equal to the average Wigner Seitz radius $R = 2.675$ a.u., in comparison to the case where the atomic radii are changed by ±5% depending on their type.

To investigate the effect of electronic correlations for the above supercells, we performed calculations using a recently developed LSDA + dynamical mean-field (DMFT) scheme.[23] Correlation effects in the valence Cr-d orbitals are included via an on-site electron-electron interaction in the form $\frac{1}{2}\sum_{i\{m,\sigma\}} U_{mm'm''m'''} c^\dagger_{im\sigma} c^\dagger_{im'\sigma'} c_{im'''\sigma'} c_{im''\sigma}$. The interaction is treated in the framework of DMFT,[24–26] with a spin-polarized T-matrix fluctuation exchange (SPTF) type of impurity solver.[27] Here, $c_{im\sigma}/c^\dagger_{im\sigma}$ destroys (creates) an electron with spin σ on orbital m on site i. The Coulomb matrix elements $U_{mm'm''m'''}$ can be computed for the particular material by taking into account the symmetry of the orbitals and the crystal structure in terms of effective Slater integrals and Racah or Kanamori coefficients.[24,28] We used the following effective Slater parameters: $F^0 = 2$ eV, $F^2 = 5.17$ eV, and $F^4 = 3.233$ eV (which results in a Coulomb-interaction of $U = 2$ eV and a Hund's rule coupling of $J = 0.6$ eV); these are in agreement with previous works.[14,17,29,30] For the exchange correlation functional the LSDA approximation was used, as we found no significant differences with respect to results using GGA.

Since static correlations are already included in the local spin-density approximation (LSDA), "double counted" terms

must be subtracted. To obtain this, we replace $\Sigma_\sigma(E)$ with $\Sigma_\sigma(E) - \Sigma_\sigma(0)$[31] in all equations of the LSDA + DMFT procedure.[24] Physically, this is related to the fact that DMFT only adds *dynamical* correlations to the LSDA result. For this reason, it is believed that this kind of double-counting subtraction "$\Sigma(0)$" is more appropriate for a DMFT treatment of metals than the alternative static "Hartree-Fock" (HF) subtraction.[32]

In the calculations we used 287 (6/4) k vectors for the Brillouin-zone integration and used a cutoff of $l_{\max} = 6$ for the multipole expansion in charge density and the potential as well as a cutoff of $l_{\max} = 4$ for the wave functions. We checked higher cutoffs for $(CrAs)_1/(GaAs)_1$ and found only negligible differences.

IV. RESULTS

A. $(CrAs)_1/(GaAs)_1$, heterostructure

The calculated LSDA band structure of $(CrAs)_1/(GaAs)_1$ displays an overall metallic behavior. It is of special interest to investigate the minority spin channel band structure shown in Fig. 4. We plot results in the energy range of -5 to 3 eV in order to distinguish between the orbitals around the Fermi level. In the tetragonal Brillouin zone the symmetry points are $\Gamma = (\pi/a)(0,0,0)$, $R = (\pi/a)(1,0,a/2)$, $A = (\pi/a)(1,1,a/c)$, $Z = (\pi/a)(0,0,a/c)$, $M = (\pi/a)(1,1,0)$, and $X = (\pi/a)(1,0,0)$. At lower energies (not shown) between -12 and -10 eV one can observe an s-like lower valence band of 2 eV in width. This is separated from the upper valence band by an interband of 3.7 eV. As one can see in Fig. 4 the bands in the energy range of -5, -1 eV are mainly hybridized As-p and Cr-d orbitals. At energies around $E_F - 1$ eV the As-p states are hybridized with Cr-d_{xz} and are situated at higher energies at the Z point, with a higher As-p weight. In comparison at the top of the valence band in the Γ point a larger weight is visible for Cr-d_{xz} states. Here, the As-p contribution is significantly reduced.

States around and just above the Fermi level also show interesting features. As we discussed above due to symmetry reduction, the X point along $\mathbf{k}_z$ of the bulk FCC zone folds over to the Γ point of the heterostructure zone. Since the lowest conduction band for the minority spin spin of bulk CrAs is situated at lower energy than the conduction band edge of bulk GaAs at the Γ point, one would expect that in the $(CrAs)_1/(GaAs)_1$ heterostructure the lowest states just above the Fermi level are an X-like CrAs band. It is clearly seen in Fig. 4 that this is not the case; the Fermi level is being crossed by Cr-d_{xy} as well as d_{z^2-1} orbitals. Note that for precisely this lattice parameter the bulk CrAs and, equivalently, the $(CrAs)_1/(CrAs)_1$ is half-metallic. Therefore the presence of GaAs determines that Cr-d_{xy} and d_{z^2-1} orbitals from the CrAs—which constitutes the "interface-layer"—to cross the Fermi level. We have performed self-consistent total energy calculations for a fixed volume of the unit cell (lattice parameter $a = 5.75$ Å) as a function of bond length, more precisely as a function of the distance between Cr-As and Ga-As atoms along the stacking direction $\delta = z_{As} - z_{Cr}$ which provides information concerning the stability of the GaAs layers with respect to the CrAs ones. In addition this analysis provides also the evolution of the Cr-d_{xy} states within the minority spin gap. As one can see in Fig. 5 within the LSDA a larger Cr-As bond length (increasing z_{As}) and smaller GaAs bond favor half-metallicity. The results of the total energy calculations show that the equilibrium bond length is realized for the distance of $\delta \approx 0.34$ for which a metallic

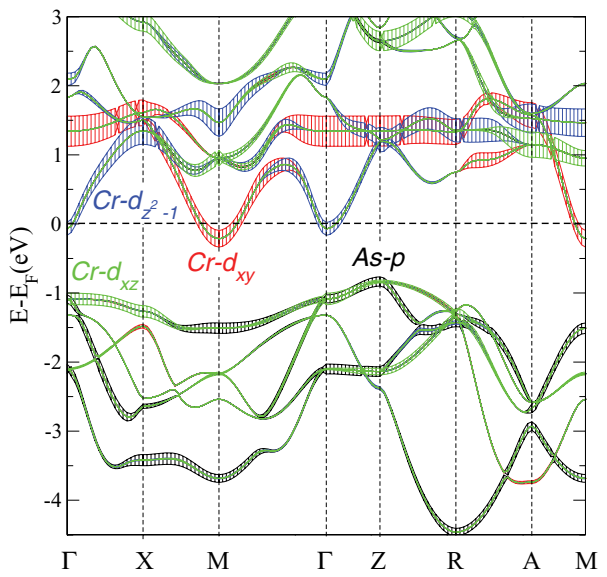

FIG. 4. (Color online) LSDA minority spin bands for $(CrAs)_1/(GaAs)_1$ along the symmetry points in the tetragonal Brillouin zone. Bands are decorated according to dominant orbitals character. The top of the valence band has mainly an As-p character (black), while the bottom of the conduction band has a Cr-d_{xy} (red) character. Cr-d_{xy} and d_{z^2-1} (blue) orbitals cross the Fermi level.

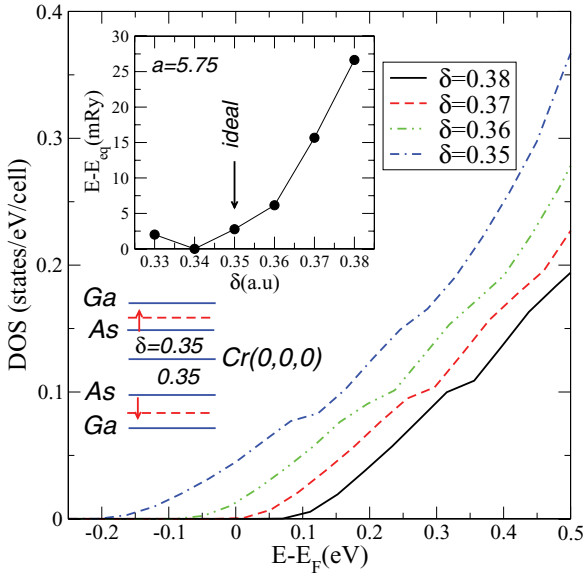

FIG. 5. (Color online) Evolution of LSDA-Cr-d_{xy} minority spin density of states of $(CrAs)_1/(GaAs)_1$ for different distances ($\delta = z_{As} - z_{Cr}$) between As and the Cr layer at fixed volume of the unit cell. The inset shows a plot of the energy (measured with respect to the equilibrium energy E_{eq}) versus δ. As one can see, at the optimal $\delta = 0.34$ the minority spin gap is closed and the heterostructure is metallic.

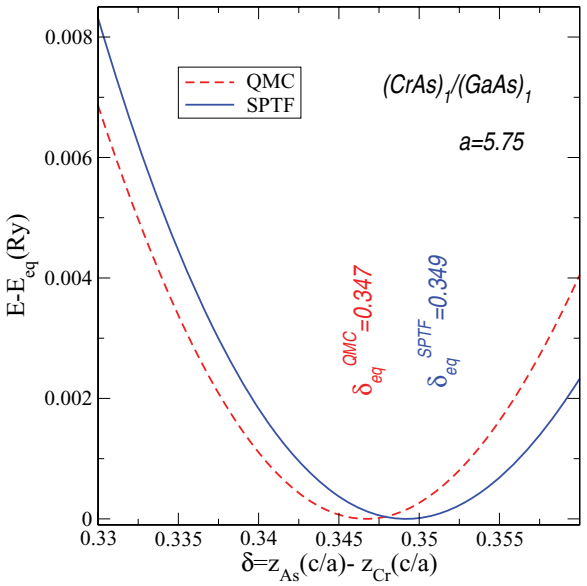

FIG. 6. (Color online) Total energies for different displacements of GaAs layer with respect the the CrAs layer in the $n = 1$ heterostructure computed within SPTF (blue solid line) and QMC (red dashed line) solvers of the DMFT, for $U = 2$ eV, $J = 0.6$ eV.

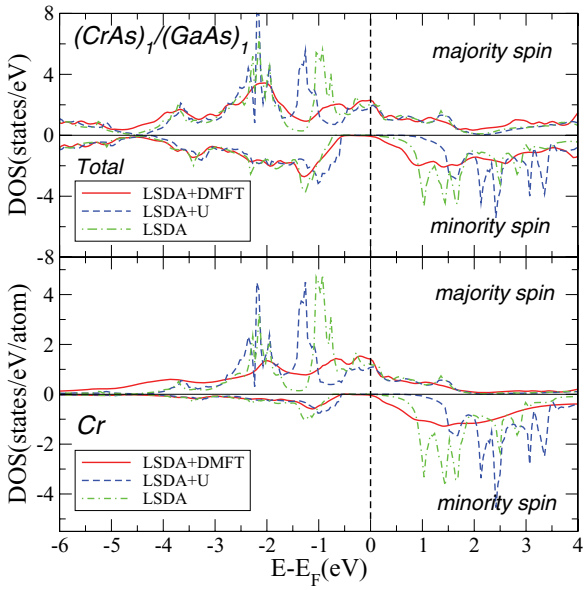

FIG. 7. (Color online) Total and Cr density of states obtained by LSDA (green dash-dotted line), LSDA + U (blue dashed line), and LDA + DMFT (red solid line) for $(CrAs)_1/(GaAs)_1$. Results obtained for the ideal $\delta = 0.35$.

$(CrAs)_1/(CrAs)_1$ heterostructure is obtained. We have checked that LSDA + U calculations with $U = 2$ eV and $J = 0.6$ eV provide the similar value for the equilibrium distance.

Similar calculations were performed, including correlation effects captured by DMFT using two different many-body solvers. In Fig. 6 we show the comparison between the calculations performed using the SPTF and the QMC–Hirsch-Fye[33] solvers. The contribution to the total energy coming from correlations was computed within the LSDA + DMFT-SPTF as an additional Galitskii-Migdal-type contribution $\frac{1}{2}\mathrm{Tr}\hat{\Sigma}\hat{G}$,[23,34] while the interaction energy within the LSDA + DMFT-QMC is computed from the double occupancy matrix $\langle \hat{n}_{im\sigma}\hat{n}_{im'\sigma'}\rangle$.[35–38] As one can see in Fig. 6 the two numerical results are in good agreement. Including correlation effects the equilibrium distance between the GaAs and the CrAs planes approaches the ideal value of $\delta = 0.35$ (corresponding to the FCC structure), thus distortions are not favored in this case. Therefore, in what follows we shall consider the ideal structure with equidistant GaAs and CrAs planes within the supercells. Because of the large supercell the following many-body results were obtained using the SPTF solver which implements the fully rotational invariant interaction discussed in the previous section.

In Fig. 7 we compare noncorrelated (LSDA), mean-field local but static correlations (LSDA + U), with dynamic (LSDA + DMFT) results. All calculations accounting for correlations were performed for the same values of the Coulomb parameter $U = 2$ eV and $J = 0.6$ eV. The minority spin gap opens within the LSDA + U calculation, in contrast to the LSDA + DMFT results where spectral weight is present in the minority spin gap. As one can see in Fig. 7 in the total density of states (upper panel) the Cr states play the dominant role. In the occupied part of the majority spin channel, the LSDA states around $E_F - 1$ eV are slightly shifted toward lower energies in LSDA + U, while in LSDA + DMFT the same states are shifted toward the Fermi level, although the spectral weight is considerably reduced. At the Fermi level, similar values for the density of states are obtained in both mean-field calculations, while a slightly larger values are obtained including dynamic correlations. For the total density of states, $E_F \pm 1$ eV is the energy range were significant differences can be seen. These differences are attributed to Cr density of states shown in the lower panel of Fig. 7.

The LSDA results give a magnetic moment close to an integer 2.99 μ_B and by including U at the mean-field level

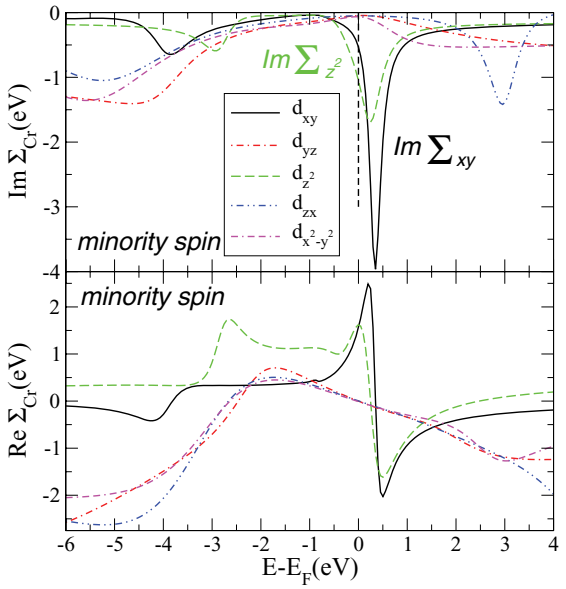

FIG. 8. (Color online) Real and imaginary part of the self-energies for Cr orbitals in the $n = 1$ heterostructure. Large values of $\Im\Sigma$ for Cr-d_{xy} (black solid line) and -d_{z^2-1} (dashed line) just above the Fermi level are related to the occurrence of NQP states.

an integer magnetic moment of 3 μ_B and a gap of 0.94 eV is obtained. The DMFT density of states is shifted toward E_F, with states just above the Fermi level. Despite their slight spectral weight close to the Fermi level, the magnetic moment has a noninteger value of 2.88 μ_B. We attribute this reduction of the magnetic moment to the appearance of nonquasiparticle states. To discuss further this effect we plot in Fig. 8 the imaginary (real) part of minority self-energy for all Cr-d orbitals. One can see a strong imaginary part associated with a strong energy dependence of the real part predominantly in Cr-d_{xy} and Cr-d_{z^2} orbitals just above the Fermi level which allows us to identify the character of nonquasiparticles states.

The presence of NQP states have been shown previously in the bulk CrAs calculations.[14] Their position in bulk is situated at higher energies above the Fermi level, in comparison with $(CrAs)_1/(GaAs)_1$, so no tails cross the Fermi level and an integer magnetic moment of 3 μ_B is obtained at finite temperatures. From the above results we conclude that the presence of GaAs layers triggers the presence of "interface" Cr-d_{xy} and Cr-d_{z^2-1} states with very small spectral weight within the minority spin channel at the Fermi level. In the presence of correlations NQP states are formed on these orbitals.

B. $(CrAs)_n/(GaAs)_n$ heterostructure, with $n = 2, 3$

For $n = 2$ the two Cr atoms are equivalent, while the As atoms in this heterostructure are shared either by two Cr atoms, two Ga atoms or one Cr and one Ga atom. In this case the heterostructure can be viewed as two $(CrAs)_1/(GaAs)_1$ interfaces coupled to the GaAs or CrAs end of the layers. Increasing the heterostructure further to $n = 3$ makes that Cr atoms become inequivalent, having one inner Cr layer and two equivalent outer Cr layers.

For the $(CrAs)_n/(GaAs)_n$ heterostructures with $n = 2,3$ a self-consistent LSDA calculation yields a half-metallic solution with an integer magnetic moment of 3 μ_B per Cr atom. The minority spin gap is 0.94 eV for $n = 2$ and 0.75 eV for $n = 3$. The minority spin gap is 0.94 eV for $n = 2$ and 0.75 eV for $n = 3$. Within LDA + U, the gap is slightly enlarged to 1.1 eV ($n = 2$) and 0.93 eV ($n = 3$), while the values for the magnetic moments remain unchanged.

DMFT results for $n = 2$ show in the majority spin channel a redistributions of spectral weight: The LSDA/LSDA + U peak at $-1/-1.5$ eV is shifted to lower energies, where new structures appear at higher bonding energies around -5 eV. At the Fermi level all three methods gives a similar value for the density of states. In the minority spin channel NQP states are visible just above the Fermi level, while below E_F the band offset is similar to the LSDA value. In Fig. 9 one can compare the overall correlation effects captured at different levels. Within LSDA + U, the gap is further increased as the bandwidth shrinks. On the other hand, dynamic correlations reduce the gap and enlarge the bandwidth, creating high-bond energy states and evidence the presence of correlation induced many-body states in the close vicinity of the Fermi level. Similar results are obtained for $n = 3$. The computed values of the magnetic moment are 5.96 and 8.99 μ_B for $n = 2$ and $n = 3$ respectively at 200 K. At 300 K magnetic moments do not change significantly $\mu_{n=2/3} = 5.97/8.98$ and the spin polarization computed at E_F is again almost temperature

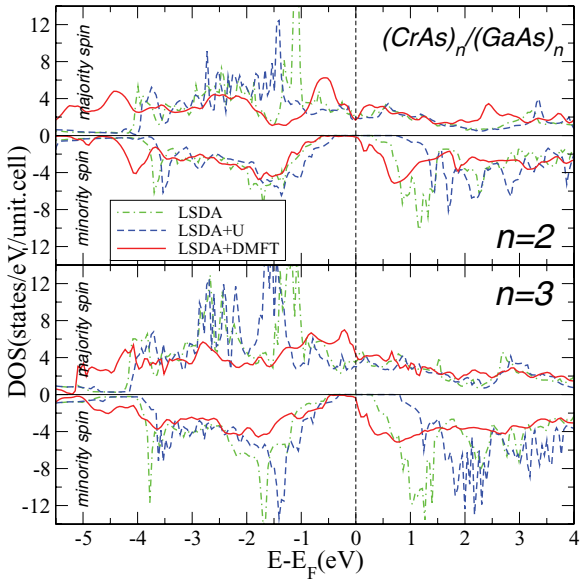

FIG. 9. (Color online) Total density of states for $(CrAs)_n/(GaAs)_n$ heterostructures for $n = 2$ and 3. LSDA (green dash-dotted line) and LSDA + U (blue dashed line) calculation yield a half-metallic state. DMFT (red solid line) results suggest the existence of NQP states just above the Fermi level with a very small spectral weight at E_F.

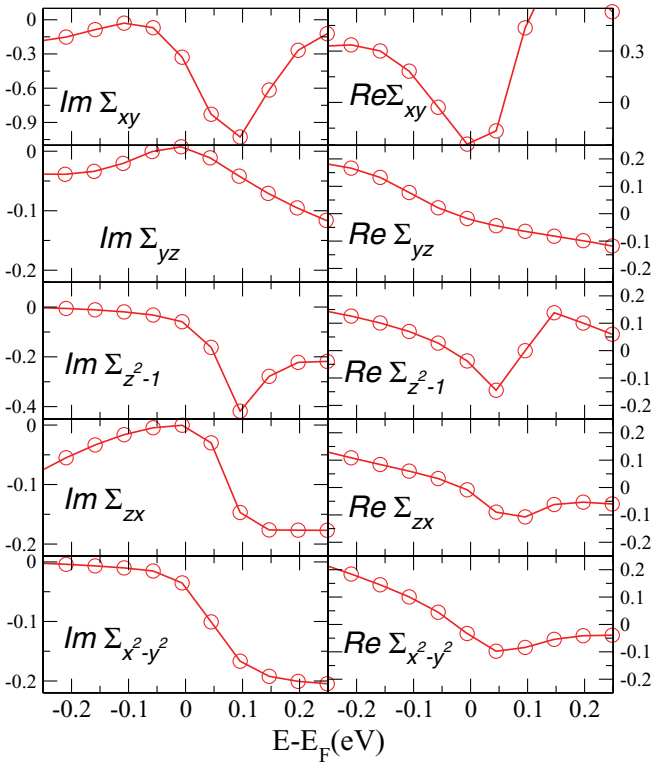

FIG. 10. (Color online) Atom and orbital resolved minority spin self-energies for $(CrAs)_2/(GaAs)_2$ heterostructure for $U = 2$ eV, $J = 0.6$ eV, and $T = 200$ K. ImΣ/ReΣ are plotted on the left/right column.

independent and has the values of $P^{n=2}_{\mathrm{DMFT}} \approx 0.76$ and $P^{n=3}_{\mathrm{DMFT}} \approx 0.71$.

As a consequence of geometrical relations between the heterostructures with $n = 1$ and $n = 2$ it is expected that also correlation effects would not different significantly. In Fig. 10 we show the layer- and orbital-resolved imaginary part of the minority spin self-energy for the heterostructure with $n = 2$. The self-energy plots contain always a single curve because of the equivalence of Cr atoms. In comparison to Fig. 8 one can see again that the Cr-d_{xy} and Cr-d_{z^2-1} states would present similar departures from the usual Fermi liquid description, although in this case the amplitude of the self-energy anomaly above E_F is reduced. This reduction can be attributed to the fact that increasing n by adding layers allows for hybridization of CrAs-GaAs layers which softens the self-energy anomaly present in the single correlated magnetic Cr layer in the $n = 1$ heterostructure.

In Fig. 11 we present the minority spin imaginary and real parts of the Cr1 (inner layer) and Cr2 (interface layer) self-energies. To analyze the correlation effects taking place for different n, we discuss a comparison of the energy dependence of the single particle self-energies in Figs. 8, 10, and 11. The visible differences are meaningful from a physical point of view as a results of the increasing number of Cr layers that can couple with increasing n. For $n = 1$ the system consists of a correlated single magnetic layer, for which the self-energy apparently deviates from the Fermi liquid description. For $n = 2$ two such Cr correlated layers couple and the self-energy anomalies are softened. Finally, the result for $n = 3$ does not show anomalous features in the energy dependence of the self-energy. On looking for small energies around the Fermi level, one can qualitatively discuss the quasiparticle lifetime or its inverse the scattering rate $1/\tau_{\mathbf{k}} \propto -\Im\Sigma(E_F)$. In comparing directly Figs. 10 and 11 the curvature of $\Im\Sigma$ is much larger for $n = 2$ than for $n = 3$. It is also important to note that for $n = 3$ the curvature is considerably larger for the interface layer than for the inner layer. The above qualitative analysis of the energy dependence of the self-energy curves suggest clearly that at the interface correlation effects are more important leading to NQP sates for the $n = 1$ and $n = 2$ cases, while for $n = 3$ Cr-d states can be described by regular quasiparticle states.

In order to study the band edges of the minority spin channel, we investigate the character (angular-momentum composition) of the electronic states below and above E_F. As discussed above, the bottom of the conduction band consists of NQP states situated just above E_F, while the top of the valence band is predominantly As-p character. We now discuss the contributions of As-p states originating from different As layers to the top of minority spin valence band. Figure 12 shows the As-p contributions to the top of the valence band as a function of numbers of layers. As the distance between the transition metal monolayer and As monolayer increases, the As-p character continues to increase. At the same time, the difference between values from different monolayers decreases. These results suggest that the As layer situated closer to the transition metal has its electrons confined by the p-d hybridization. At larger distances, hybridization decreases, and more p character is available to form the top of the valence band.

At larger temperatures, the As-p relative contribution to the top of the valence band slightly decreases within the

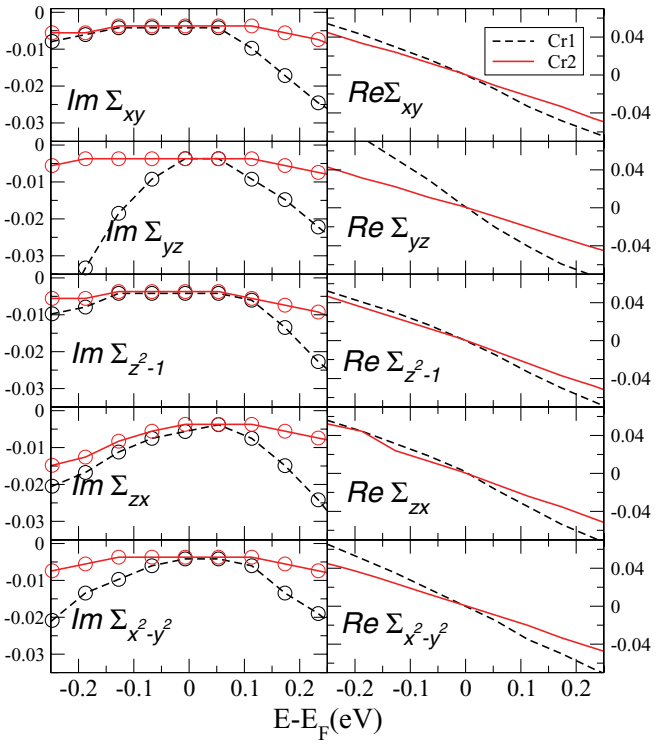

FIG. 11. (Color online) Atom and orbital resolved minority spin self-energies for $(CrAs)_3/(GaAs)_3$ heterostructure for $U = 2$ eV, $J = 0.6$ eV, and $T = 200$ K. $\mathrm{Im}\Sigma/\mathrm{Re}\Sigma$ are plotted on the left/right column. Cr1(interface)/Cr2(inner) atoms are plotted in dashed (black)/solid (red). An almost linear behavior can be seen for $\mathrm{Re}\Sigma$ for inner type atoms. Possible kinks are visible for $\mathrm{Re}\Sigma_{\mathrm{Cr1}}$.

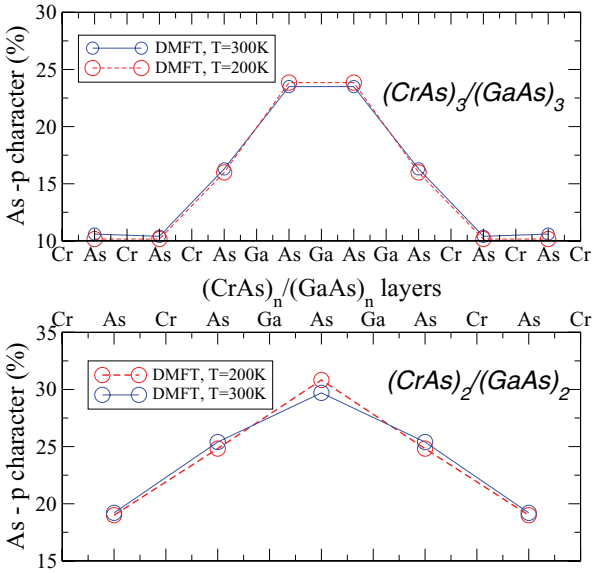

FIG. 12. (Color online) Relative contribution (in percentage points) of As-p states to the valence band maxima for each layer of the two superlattices ($n = 2$ and 3). Results are shown for $(CrAs)_n/(GaAs)_n$ heterostructures with $U = 2$ eV, $J = 0.6$ eV, and $T = 200$ K (red dashed line), 300 K (blue solid line).

GaAs layers and increases for As contained within the CrAs layers. This demonstrates that the confinement of carriers seen already at the LSDA level, i.e., the valence-band top almost confined on the GaAs region, and the bottom of conduction band confined on CrAs, is not significantly changed by finite temperature electronic correlations. Therefore the electrons and holes remain separated in different regions of the real space.

V. SUMMARY

Heterostructures made of layers of Heusler half-metals alternated with semiconductors suffer from the presence of interface states within the half-metallic gap which strongly reduce the possibility of spin-polarized current injection. From previous theoretical studies it is known that the only case when half-metallicity is retained is the case of a NiMnSb(111)/CdS(111) interface formed between Sb and S atoms.[39] Alternative options are provided by zinc-blende half-metals due to their affinity with the structure of zinc-blende semiconductors. In the present article we have performed combined electronic structure and many-body calculations for short-period $(CrAs)_n/(GaAs)_n$ heterostructures, with $n \leqslant 3$ having a lattice parameter of $a = 5.75$ Å. For $n = 1$ we investigated the properties of a single-interface layer and demonstrate that Cr-d_{xy} and Cr-d_{z^2-1} states that cross the Fermi level acquire a nonquasiparticle character in the presence of correlations. Our results demonstrate that heterostructures for $n = 2,3$ feature magnetizations deviating by less than 2% from the integer half-metallic values at temperatures close to room temperature $T = 200, 300$ K. The computed finite temperature polarizations deviate significantly from the expected 100%. However, we believe that these values $P_{\mathrm{DMFT}}(E_F) \approx 75\%$, that are far larger then values for other (semi-)Heuslers are still sufficient to make such a heterostructure interesting for future spintronic applications. In addition, we have investigated the character of the minority spin states around the Fermi level. While the top of the valence band mainly consists of As-p electrons localized on GaAs layers, the bottom of the conduction band is mainly determined by many-body induced NQP states having Cr-d character. This results, therefore, suggest that carriers remain separated among different layers in these heterostructures.

ACKNOWLEDGMENTS

We are grateful to D. Vollhardt for useful discussions. This work was supported by the Austrian science fund (FWF project P21289-N16) and by the cooperation project "NAWI Graz" (F-NW-515-GASS).

[1] R. A. de Groot, F. M. Mueller, P. G. van Engen, and K. H. J. Buschow, Phys. Rev. Lett. **50**, 2024 (1983).
[2] M. I. Katsnelson, V. Y. Irkhin, L. Chioncel, A. I. Lichtenstein, and R. A. de Groot, Rev. Mod. Phys. **80**, 315 (2008).
[3] Y.-J. Zhao and A. Zunger, Phys. Rev. B **71**, 132403 (2005).
[4] H. Akinaga, T. Magano, and M. Shirai, Jpn. J. Appl. Phys. **39**, L1118 (2000).
[5] M. Mizuguchi, H. Akinaga, T. Manago, K. Ono, M. Oshima, M. Shirai, M. Yuri, H. J. Lin, H. H. Hsieh, and C. T. Chen, J. Appl. Phys. **91**, 7917 (2002).
[6] K. Nagao, M. Shirai, and Y. Miura, J. Appl. Phys. **95**, 6518 (2004).
[7] H. Akinaga and M. Mizuguchi, J. Phys. Condens. Matter **16**, S5549 (2004).
[8] S. Gopalan, N. E. Christensen, and M. Cardona, Phys. Rev. B **39**, 5165 (1989).
[9] A. Continenza, S. Picozzi, W. T. Geng, and A. J. Freeman, Phys. Rev. B **64**, 085204 (2001).
[10] Y.-J. Zhao, W. T. Geng, A. J. Freeman, and B. Delley, Phys. Rev. B **65**, 113202 (2002).
[11] W.-H. Xie, Y.-Q. Xu, B.-G. Liu, and D. G. Pettifor, Phys. Rev. Lett. **91**, 037204 (2003).
[12] I. Galanakis and P. Mavropoulos, Phys. Rev. B **67**, 104417 (2003).
[13] M. Shirai, J. Appl. Phys. **93**, 6844 (2003).
[14] L. Chioncel, M. I. Katsnelson, G. A. de Wijs, R. A. de Groot, and A. I. Lichtenstein, Phys. Rev. B **71**, 085111 (2005).
[15] D. M. Edwards and J. A. Hertz, J. Phys. F Met. Phys. **3**, 2191 (1973).
[16] V. Y. Irkhin and M. I. Katsnelson, J. Phys. Condens. Matter **2**, 7151 (1990).
[17] L. Chioncel, M. I. Katsnelson, R. A. de Groot, and A. I. Lichtenstein, Phys. Rev. B **68**, 144425 (2003).
[18] L. Chioncel, H. Allmaier, E. Arrigoni, A. Yamasaki, M. Daghofer, M. Katsnelson, and A. Lichtenstein, Phys. Rev. B **75**, 140406 (2007).
[19] L. Chioncel, Y. Sakuraba, E. Arrigoni, M. I. Katsnelson, M. Oogane, Y. Ando, T. Miyazaki, E. Burzo, and A. I. Lichtenstein, Phys. Rev. Lett. **100**, 086402 (2008).
[20] M. Shirai, K. Ikeuchi, H. Taguchi, and H. Akinaga, J. Supercond. **16**, 27 (2003).
[21] H. Kino, F. Aryasetiawan, I. Solovyev, T. Miyake, T. Ohno, and K. Terakura, Physica B **329–333**, 858 (2003).
[22] M. Geshi, M. Shirai, K. Kusakabe, and N. Suzuki, Comput. Mater. Sci. **36**, 143 (2006).
[23] L. Chioncel, L. Vitos, I. A. Abrikosov, J. Kollar, M. I. Katsnelson, and A. I. Lichtenstein, Phys. Rev. B **67**, 235106 (2003).
[24] G. Kotliar, S. Y. Savrasov, K. Haule, V. S. Oudovenko, O. Parcollet, and C. A. Marianetti, Rev. Mod. Phys. **78**, 865 (2006).
[25] G. Kotliar and D. Vollhardt, Phys. Today **57**, 53 (2004).
[26] K. Held, Adv. Phys. **56**, 829 (2007).
[27] M. I. Katsnelson and A. I. Lichtenstein, Eur. Phys. J. B **30**, 9 (2002).
[28] M. Imada, A. Fujimori, and Y. Tokura, Rev. Mod. Phys. **70**, 1039 (1998).
[29] L. Chioncel, E. Arrigoni, M. I. Katsnelson, and A. I. Lichtenstein, Phys. Rev. Lett. **96**, 137203 (2006).
[30] L. Chioncel, P. Mavropoulos, M. Ležaić, S. Blügel, E. Arrigoni, M. I. Katsnelson, and A. I. Lichtenstein, Phys. Rev. Lett. **96**, 197203 (2006).
[31] A. I. Lichtenstein, M. I. Katsnelson, and G. Kotliar, Phys. Rev. Lett. **87**, 067205 (2001).
[32] A. G. Petukhov, I. I. Mazin, L. Chioncel, and A. I. Lichtenstein, Phys. Rev. B **67**, 153106 (2003).
[33] M. Jarrell, Phys. Rev. Lett. **69**, 168 (1992).

[34]I. Di Marco, J. Minár, S. Chadov, M. I. Katsnelson, H. Ebert, and A. I. Lichtenstein, Phys. Rev. B **79**, 115111 (2009).
[35]I. Leonov, N. Binggeli, D. Korotin, V. I. Anisimov, N. Stojić, and D. Vollhardt, Phys. Rev. Lett. **101**, 096405 (2008).
[36]I. Leonov, D. Korotin, N. Binggeli, V. I. Anisimov, and D. Vollhardt, Phys. Rev. B **81**, 075109 (2010).
[37]K. Held, A. K. McMahan, and R. T. Scalettar, Phys. Rev. Lett. **87**, 276404 (2001).
[38]L. Chioncel and E. Burzo, J. Optoelectron. Adv. Mat. **8**, 1105 (2006).
[39]G. A. de Wijs and R. A. de Groot, Phys. Rev. B **64**, 020402 (2001).